ELSEVIER

Chemical Geology 221 (2005) 188–206

CHEMICAL GEOLOGY
INCLUDING
ISOTOPE GEOSCIENCE

www.elsevier.com/locate/chemgeo

Geology and stable isotope (O, H, C, S) constraints on the genesis of the Cachoeira gold deposit, Gurupi Belt, northern Brazil

Evandro L. Klein [a,*], Chris Harris [b,1], André Giret [b], Candido A.V. Moura [c], Rômulo S. Angélica [c]

[a] *CPRM/Geological Survey of Brazil, Av. Dr. Freitas, 3645, Belém-PA, CEP: 66095-110, Brazil*
[b] *Université Jean Monnet, Département de Géologie, 23, rue du Docteur Paul Michelon, 42023, Saint Etienne CEDEX-2, France*
[c] *Universidade Federal do Pará, Centro de Geociências, CP 1611, Belém-PA, CEP: 66075-900, Brazil*

Received 3 August 2004; received in revised form 29 April 2005; accepted 3 May 2005

Abstract

The Cachoeira gold deposit is one of several large (>20 tonnes Au), shear-zone hosted hydrothermal gold deposits of the Proterozoic Gurupi Belt in northern Brazil. O, H, C, and S isotope compositions of carbonate, silicate, and sulfide minerals, and from graphite and inclusion fluids from this deposit have been measured in order to infer the composition of ore-forming fluids. The data show small variation at the deposit scale, irrespective of host rock. Calculated $\delta^{18}O$ values of H_2O in the fluid in equilibrium with quartz, hydrous silicates and carbonates are, respectively, +6.2 to +12.4‰, +5.0 to +9.0‰, and +5.9 to +11.0‰ (SMOW). The δD_{H_2O} of inclusion fluids is −22‰, whereas values for chlorite and white mica are −16‰ and −20 to −28‰ (SMOW), respectively. These values are compatible with a metamorphic origin, which is in agreement with the post-metamorphic timing of the mineralization. The calculated $\delta^{13}C$ value of CO_2 of the fluid in equilibrium with the carbonates is from −9.5‰ to −12.7‰ (PDB), whereas the graphite-bearing host rocks have $\delta^{13}C$ value of graphite carbon of −29.7‰. The calculated $\delta^{34}S$ of H_2S of the fluid varies mainly between +0.7‰ and +5.5‰ (CDT), and is interpreted as reflecting a magmatic or average crustal source for sulfur. The restricted isotopic compositions indicate a relatively homogeneous fluid and deposition under restricted temperature conditions. Nonetheless, a relatively wide temperature range of 272–383 °C is estimated for the ore-bearing fluid using the quartz–dolomite oxygen isotope thermometer. Collectively, the data indicate that gold was transported as a reduced sulfur complex, by a metamorphic fluid having a near neutral pH, at relatively low $f\,O_2$. Furthermore, the data suggest that gold was deposited during the structural evolution of the associated shear zone probably as a result of sulfidation and carbonatization reactions with the Fe- and C-rich host rocks, which resulted in changes of the pH and in the redox state of the ore fluid.

Keywords: Gold; Stable isotopes; Shear zone; Gurupi Belt; Paleoproterozoic; Brazil

* Corresponding author.
E-mail address: eklein@be.cprm.gov.br (E.L. Klein).
[1] Present address: Department of Geological Sciences, University of Cape Town, Rondebosch 7700, South Africa.

0009-2541/$ - see front matter © 2005 Elsevier B.V. All rights reserved.
doi:10.1016/j.chemgeo.2005.05.003

1. Introduction

The Gurupi Belt in northern Brazil hosts several gold deposits and small, undeveloped occurrences. The Cachoeira deposit, located about 180 km east of Belém (Pará State) in the northwestern portion of the Gurupi Belt, is one of the most important deposits in the area, along with Cipoeiro, Chega Tudo, Montes Áureos and Serrinha (Fig. 1). The deposit is in fact a gold camp formed by tens of discontinuous ore bodies, which include isolated quartz veins, vein systems, hydrothermally altered host rocks and stockworks, distributed along an area of approximately 3.5 km × 1.5 km (Fig. 2). The historical production, since the 19th century, is about 1.2 tonnes Au (Bettencourt et al., 1991). Over the past two decades different mining companies have exploited several individual targets where alluvial, supergene, and hard rock ore have been detected. Geologic resources total 20 tonnes Au from which the primary mineralization, with grades varying from 1.7 to 4.4 g/t Au, contributes with over 17 tonnes (CCO and Xopotó Mining Co., internal reports).

Some aspects of the geologic context of the Cachoeira deposit have already been addressed in previous works (Bettencourt et al., 1991; Trarbach and Kotschoubey, 1991), however, several aspects concerning the genetic model still remained uncertain. These include: the hydrothermal paragenesis; the relative timing of gold mineralization with respect to metamorphism and deformation; the absolute timing of mineralization; the composition of the mineralizing fluid; the physico-chemical (P–T–fO_2) conditions of ore formation; and the sources for fluid components. In this paper we discuss some of these aspects. We outline the geologic features of the Cachoeira deposit, based on recent geologic mapping and information from drill cores, and provide petrographic and stable isotope (O, H, C, S) data on minerals associated with the hydrothermal alteration linked to gold mineralization. The results allow us to estimate the fluid composition, the formation temperature of the ore, the possible sources for the hydrothermal fluids, and speculate on the mechanisms for gold transport and precipitation.

2. Geologic setting

The Cachoeira deposit is hosted by rocks belonging to the Gurupi Belt. This is an elongated plutono-metamorphic belt that borders the south–southwestern margin of the São Luis Craton (Fig. 1). The craton is composed of two major generations of calc–alkaline granitoids having single zircon Pb-evaporation ages ranging from 2165 ± 2 Ma to 2149 ± 5 Ma (Klein and Moura, 2001, 2003), and of younger peraluminous granitoids of 2086 ± 10 Ma (Palheta, 2001). These granitoids intruded a metavolcano-sedimentary sequence dated at 2240 ± 5 Ma (Klein and Moura, 2001). Cratonization occurred at about 1900 Ma, as deduced from Rb–Sr and K–Ar data on rocks and minerals (see primary references and review in Klein and Moura, 2001).

The boundary between the craton and the Gurupi Belt is gradational and defined by the Tentugal shear zone (Hasui et al., 1984), which comprises a ~120 km long and 15–30 km wide corridor of highly strained rocks (Hasui et al., 1984; Costa et al., 1988; Ribeiro, 2002). This terrane-bounding sinistral strike-slip shear zone is an important metallogenic feature, since all known gold deposits and occurrences of the Gurupi Belt are located within this deformation zone (Fig. 1).

The Gurupi Belt consists of NNW- and SSE-trending supracrustal sequences, which are tectonically intercalated with amphibolite–facies gneisses and intruded by different generations of plutonic rocks. The supracrustal sequences may be subdivided into at least three successions (Fig. 1). The Chega Tudo Formation consists of an alternation of felsic to mafic volcanic and clastic sedimentary rocks that underwent metamorphism under greenschist to lower-amphibolite conditions. Most of the rocks show a well-developed schistosity and/or mylonitic fabric that dip generally to the SW at moderate to high angles. They are locally folded, especially within the Tentugal shear zone. Two felsic metavolcanic rocks yielded Pb-evaporation zircon ages of 2148 ± 1 Ma and 2160 ± 3 Ma (Klein and Moura, 2001) interpreted as the crystallization ages of the volcanic protoliths. The Gurupi Group comprises metasedimentary rocks of sub-greenschist to amphibolite metamorphic conditions, and is tentatively positioned in the Paleoproterozoic, based on supposed

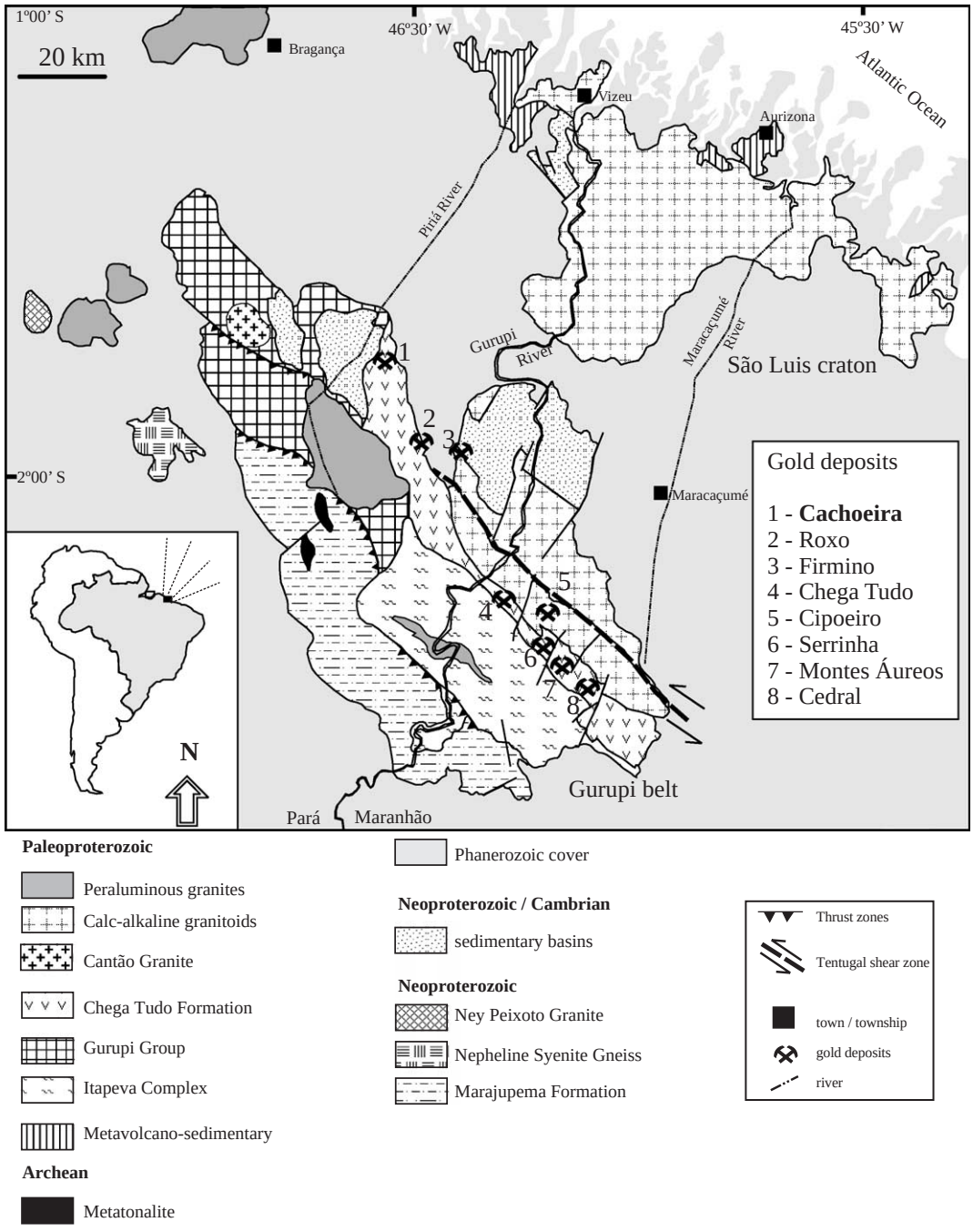

Fig. 1. Simplified geological map of the São Luis Craton and Gurupi Belt, showing the location of the Cachoeira and other gold deposits.

intrusion relationships with granitoids of 2085–2159 Ma (Costa, 2000; Palheta, 2001). The third supracrustal sequence, Marajupema Formation, is comprised of coarse-grained schists and aluminous quartzites of amphibolite facies, having a maximum sedimentation age of about 1100 Ma (Klein, 2004).

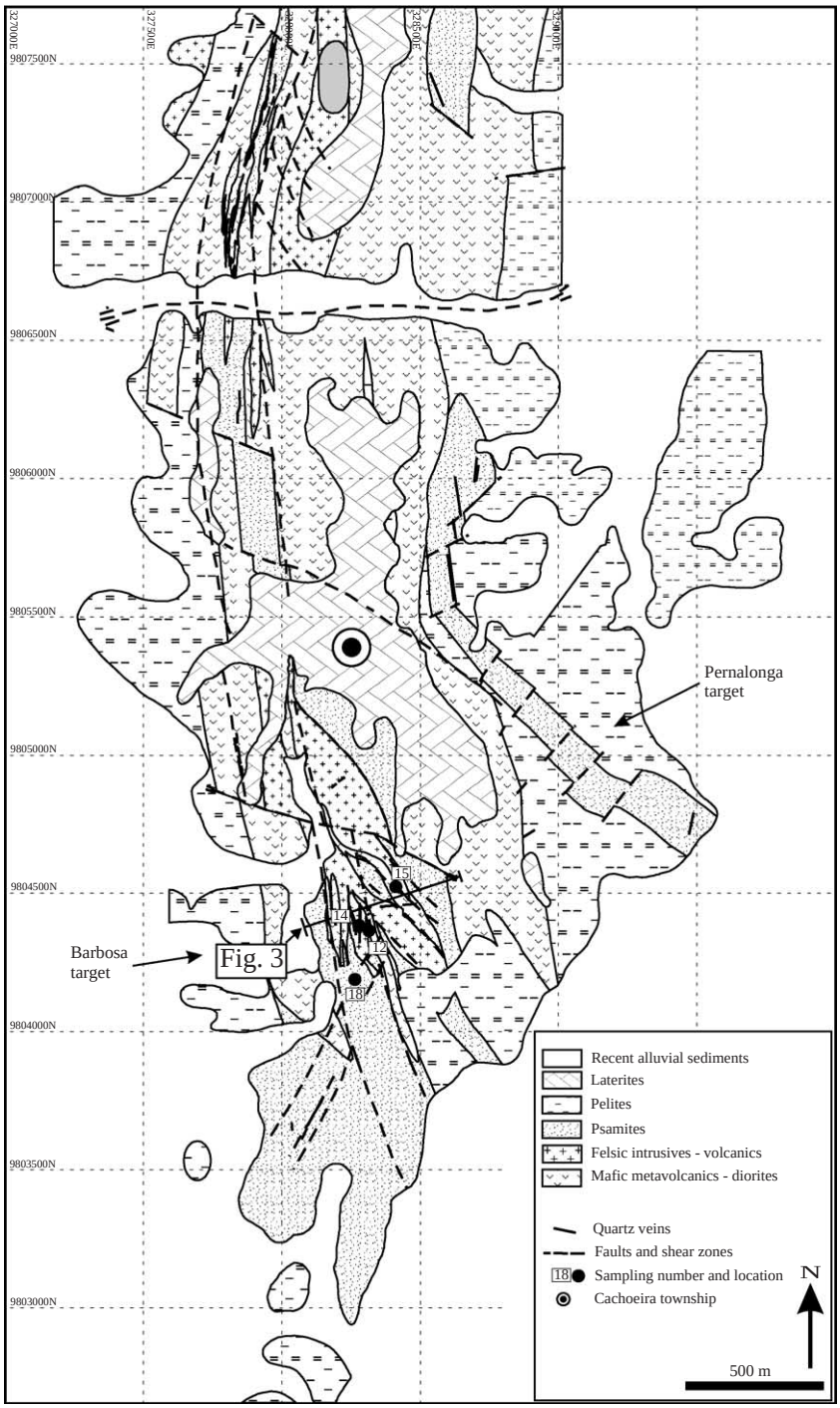

Fig. 2. Geological map of the deposit area showing the location of the drilling sites sampled for this study and of the location of the cross-section SW–NE detailed in Fig. 3.

Orthogneisses of medium- to higher-amphibolite facies with localized migmatization (Itapeva Complex) are in tectonic contact with the supracrustal successions. Single-zircon Pb-evaporation dating of a tonalitic gneiss revealed variable zircon ages. The oldest (2135 ± 4 Ma) has been interpreted as being the minimum age of the igneous protolith of the gneiss (Klein and Moura, 2003). Granitoids of distinct geochemical affinities and ages intrude both the supracrustal sequences and the gneisses. Cantão is a weakly and only locally deformed body of monzogranite that supposedly intruded the supracrustal rocks of the Gurupi Group (no field relationships are visible) at 2159 ± 13 (Palheta, 2001), since it contains enclaves of metavolcano-sedimentary rocks. Peraluminous, muscovite-bearing granites are relatively widespread, and show variable effects of deformation, from a weak schistosity to a penetrative mylonitic fabric. Lead-evaporation and conventional U–Pb zircon ages of these granites vary between 2100 and 2060 Ma, with inherited zircons recording ages in the 2325–2459 Ma range, while the T_{DM} model ages vary between 2.09 and 3.23 Ga (Palheta, 2001; Klein, 2004). The Ney Peixoto Granite is also a peraluminous granite, but with zircon age of 549 ± 4 Ma (Palheta, 2001).

An isolated body of a metamorphosed (gneissic) nepheline–syenite crops out in the middle of the Phanerozoic sedimentary cover (Fig. 1). This rock intruded at 730 Ma (Klein, 2004) and underwent amphibolite–facies metamorphism probably between 580–550 Ma. Continental clastic sedimentary rocks (arkose, pelite, conglomerate), weakly foliated and locally metamorphosed at sub-greenschist conditions, occur in the northern sector of the Gurupi Belt (Abreu et al., 1980; Pastana, 1995; Fig. 1). The depositional age is probably close to the Neoproterozoic/Paleozoic boundary, by comparison with the Igarapé de Areia Formation of the São Luis Craton that shows detrital zircons with ages in the 600–650 Ma range (Pinheiro et al., 2003). Additionally, Rb–Sr and K–Ar ages of rocks from various lithostratigraphic units also yielded ages varying from 520 to 670 Ma (Hurley et al., 1968; Almeida et al., 1968; Villas, 1982; Klein and Moura, 2001, and references therein).

As a whole the Gurupi Belt records at least two orogenic episodes: the first occurred in the Paleoproterozoic and is well defined by the collision-type granites of 2100–2080 Ma; the second took place in the Neoproterozoic and is evidenced by the gneissic fabric and the amphibolite–facies metamorphism of the nepheline–syenite, and by the intrusion of the peraluminous granite at 549 Ma. In addition, the Rb–Sr and K–Ar mineral ages of rocks that formed in the Paleoproterozoic reinforce the imprinting of this Neoproterozoic activity.

3. Geology of the Cachoeira gold deposit

3.1. Host rocks

The host rocks of the deposit consist of a metavolcano-sedimentary sequence (Barbosa target), assigned to the Chega Tudo Formation, here dominated by mafic and felsic metaigneous rocks, and a metasedimentary unit (Pernalonga target) of equivocal stratigraphic position (Gurupi Group or Chega Tudo Formation?). These sequences occur as subparallel, broadly N/S-trending, elongated bodies from a few tens to hundreds of meters in thickness (Figs. 2 and 3). Rocks are variably foliated exhibiting a N/S-trending subvertical schistosity and/or mylonitic fabric.

Since the hosting succession underwent greenschist facies metamorphism, the prefix meta is implicit in the rock descriptions. The mafic and intermediate rocks comprise tuffs, basalts, andesites, chlorite schists with intercalated ultramafic rocks (chlorite–talc schist), and fine- to coarse-grained diorite. Graphite-bearing phyllites are often intercalated in this sequence. The tuffs are brown, fine-grained and generally schistose rocks. The basalts and andesites are massive to foliated and show a dark gray color, when fresh, and green when hydrothermally altered. Chlorite schists, with intercalated tuffs, are dark green rocks, probably derived from the fine-grained tuffs and volcanics in highly strained portions of the deposit. Dacites and possibly rhyodacites, either volcanic or intrusive (synvolcanic dykes?), compose the felsic unit. They show aphyric to porphyritic texture, and are often schistose and/or mylonitic, with the foliation being defined by elongated and aligned grains of white mica.

The sedimentary sequence shows a psammitic unit, composed of arkose, greywacke and tuffs, and a pelitic unit with intercalated siltstones and carbonaceous phyllites (black shale?). The arkose shows yellowish, whitish and pinkish colors and is medium- to coarse-grained

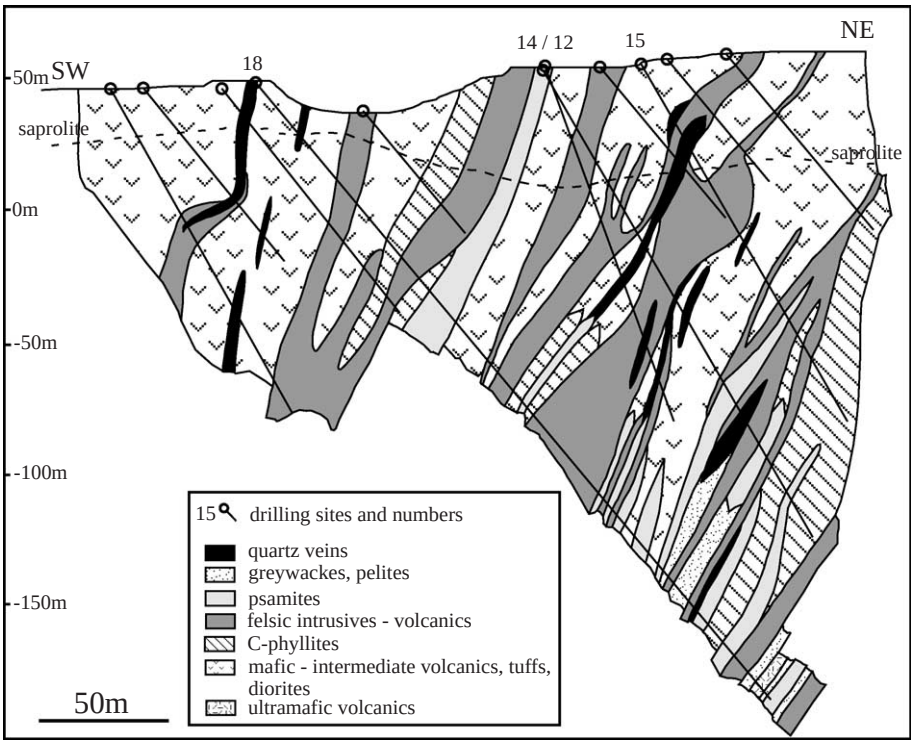

Fig. 3. Cross-section of the Cachoeira deposit. The numbered drill holes were sampled for this study. Location of the cross-section is in Fig. 2.

with conglomerate levels and magnetite bands. It is sheared but shows preserved primary cross bedding.

Although most of the rock types are to some extent mineralized, there is an apparent lithological control in localizing the more economic mineralization within mafic tuffs and coarse- to fine-grained diorites (Figs. 3 and 4). Felsic to mafic volcanic rocks, sericitic schists and carbonaceous phyllites are subordinately mineralized, whereas greywackes and arkoses are only weakly mineralized. This study concentrates in the metavolcano-sedimentary-hosted mineralization (Barbosa target).

3.2. Structure

The gold-hosting metavolcano-sedimentary sequence displays NW/SE- to N/S-trending foliation that dips at high angles to the SW, with subhorizontal stretching lineations, indicating a transpressional sinistral strike-slip regime. In the deposit area, brittle–ductile, mainly strike-slip shear zones are widespread and these have been the sites of intense fluid circulation as reflected in the widespread hydrothermal alteration. They are chiefly north- and south-trending structures that dip at high angles to the west (Figs. 2 and 3), and were subsequently reactivated as brittle faults that produced brecciated zones. East/west- and WNW/ESE-trending strike-slip faults displaced the N/S-trending structures, whereas NE/SW-striking normal faults affected mainly the sedimentary sequence (Fig. 2). Both brittle structures are late in the structural evolution of the deposit and post-date the mineralization. A considerable part of the mineralized veins and other ore shoots cluster between segments of a curvilinear, but overall N/S-trending fault zone (Fig. 2). The ductile deformation imparted a schistose and/or mylonitic fabric to the rocks, depending on their composition, competency, and position in relation to the deformation zones.

3.3. Hydrothermal alteration and mineralization

Weathering has led to the formation of supergene ore extending to depths that locally exceed 140 m.

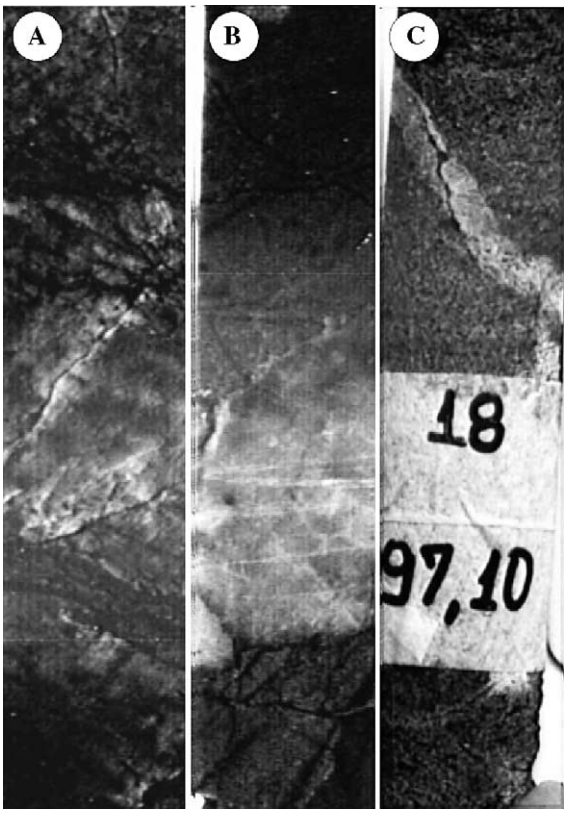

Fig. 4. Selected features of the hydrothermal alteration at Cachoeira. (A) Altered diorite showing bleached haloes around small fractures. (B) Fine-grained felsic volcanic rock cut by quartz veinlet. (C) Microdiorite cut by quartz veinlet. Drill cores are 3 cm wide.

Supergene gold is very fine-grained, hosted in saprolites and gossans and is associated with enhanced contents of Ag and As (Trarbach and Kotschoubey, 1991). Several mineralized zones in hard rocks (not affected by surface weathering) have been intersected by drill holes in both targets, and individual zones are mostly between 7 and 17 m thick and may total 20 to 54 m in different sections. Gold grades range from 1.0 to 2.3 ppm in the volcano-sedimentary sequence (Barbosa target) and from 0.3 to 0.8 ppm in the arkoses (Pernalonga target).

The hydrothermal alteration of the volcano-sedimentary sequence produced a broadly constant mineral assemblage and is comprised of a pervasive and three veining stages (Fig. 5). The first stage consists of milky to smoky quartz (± sulfide) veins (Fig. 6A), showing variable thickness (average 60 cm). These veins are subparallel to the local N/S trend and, in places, they are folded. Under the microscope, the quartz crystals show highly undulose extinction, deformation lamellae and widespread dynamic recrystallization (Fig. 6B), indicating strong effects of ductile deformation. This deformation resulted in the elimination and/or modification of most of the primary fluid inclusions in the studied samples, and the remaining inclusions are too small for conventional microthermometric investigation. The veins show also some brecciation imparted by a late brittle deformation. Possibly, more than one stage of veining is included here, but these are impossible to distinguish (see Timing of gold mineralization).

The pervasive alteration assemblage comprises variable proportions of quartz, carbonate, albite, and sulfide minerals that overprint the metamorphic paragenesis and show a dominantly oriented pattern (Fig. 6C and D), indicating a post-metamorphic and syntectonic character. Fine-grained chlorite and white mica are also present, but they are neither voluminous nor ubiquitous. The carbonate mineral is dolomite, as determined by X-ray diffraction, and it may attain >30 vol.% of the veins. Albite is ubiquitous and abundant, locally attaining 70 vol.%. The sulfide minerals are pyrite and subordinate arsenopyrite, occurring in variable proportions, ranging from 1 to 5 vol.% (occasionally up to 8–10 vol.%). They occur either isolated or in close association, forming disseminations or stringers. The pyrite is normally fine-grained and euhedral, and the grains cut the foliation, in keeping with a post-metamorphic origin. Nevertheless, local signs of deformation, such as fracturing and rotation, are observed. The arsenopyrite is medium-grained, anhedral to euhedral, rhomb-shaped or prismatic, and some grains show twinning. In places, the alteration is more evident around small fractures, where it forms bleached halos (Fig. 4). Narrow quartz-only and quartz-dominated composite veinlets (± carbonate ± albite ± sulfide) crosscut the pervasive assemblage (Fig. 6C) and the thicker quartz veins (Fig. 6A), showing variable orientations. The carbonate is also dolomite that forms up to 35 vol.% of the veinlets. Sulfide minerals (pyrite, arsenopyrite) are disseminated along the veinlets. These veinlets show also effects of ductile deformation, such as undulose extinction of the quartz and albite grains, along with subgrain development (Fig. 6E). In fact,

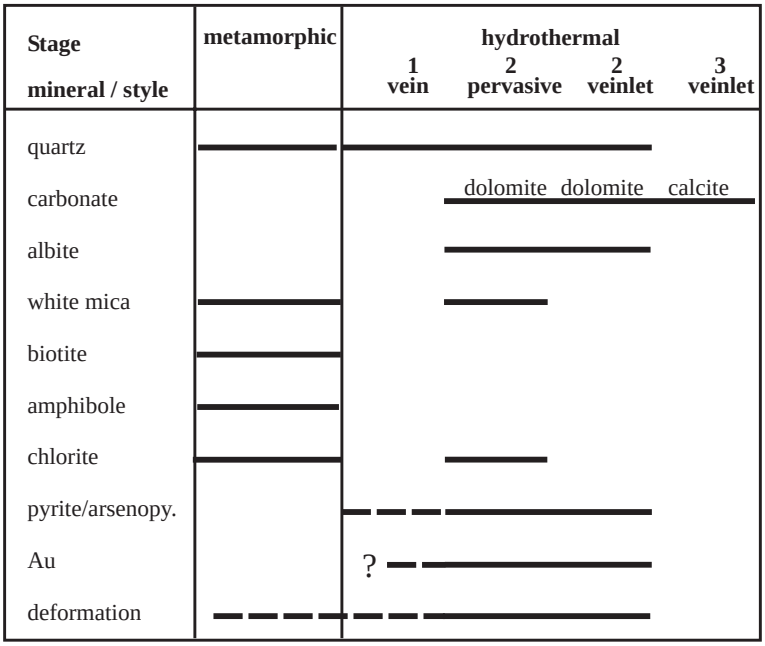

Fig. 5. Diagram showing the mineralogical composition in the metamorphic and hydrothermal assemblages at the Cachoeira deposit.

the pervasive and this second veining stage show the same mineralogical composition and likely represent a single but prolonged stage in which the pervasively altered rocks have been fractured, then the fractures have been filled with the same alteration minerals. Gold is rarely visible, occurring both in the veins and pervasive alteration, in general associated with sulfide concentrations.

The last hydrothermal stage is represented by calcite veinlets. These veinlets have not undergone plastic deformation, and they crosscut both the foliation of the host mafic volcanic rock and thin layers of foliation concordant sulfide minerals (Fig. 6F). According to Kerrich (1989), the precipitation of calcite and dolomite is sensitive to P_{CO_2}, with dolomite requiring higher P_{CO_2} conditions than calcite. At Cachoeira, the precipitation of dolomite in the main alteration stage, and of calcite towards the end of the hydrothermal activity may be accounted for by the lowering in the P_{CO_2}. This lowering could have been produced by the progressive consumption of CO_2 that reacts with the silicate minerals of the host rocks to form dolomite in the main hydrothermal stage. The dominance of mafic host rocks favors the crystallization of dolomite as well.

3.4. Timing of gold mineralization

The mesoscopic and microstructural characteristics of the quartz veins and host rocks, along with the crosscutting relationships of distinct generations of veins, faults and shear zones allow us to constrain the relative timing of vein deposition and hydrothermal alteration with respect to deformation. The thick quartz veins both crosscut and parallel the foliation defined by the pervasive hydrothermal assemblage. These veins show microstructural evidence of strong ductile deformation. The pervasive hydrothermal assemblage shows post-metamorphic and syntectonic characteristics. We consider that they have formed during the ductile deformation and are also syntectonic, but it is clear that deformation outlasted vein deposition and hydrothermal alteration. However, at least part of the veins may pre-date the main deformation, but we could not clearly distinguish them. In fact, elsewhere in the deposit, Bettencourt et al. (1991) described early en-echelon dilation veins that have subsequently been folded and reoriented to the local north/south-trending foliation. Most of the veins show brittle structures also associated with the hydrothermal alteration. It is likely that the described fea-

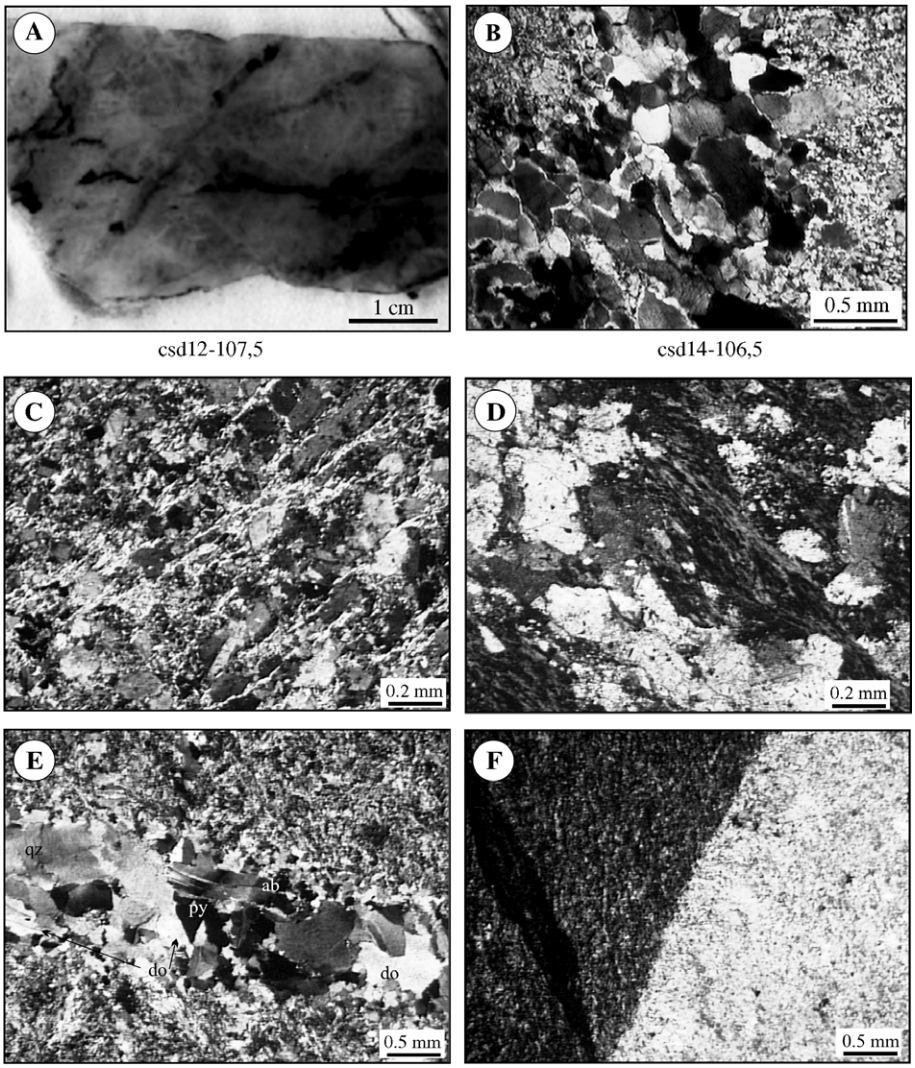

Fig. 6. Photograph (A) and crossed nicols photomicrographs (B to F) of veins and hydrothermal alteration of the host sequence in the Cachoeira deposit. A) Polished slab of a smoky quartz vein from stage-1. Crosscutting fractures are filled with stage-2 quartz–carbonate veinlets. B) Veinlet of recrystallized quartz nearly lacking of fluid inclusions. C) Stage-2 pervasive and oriented carbonate-dominated (white) and albite-rich (dark gray) alteration of a felsic metavolcanic rock. D) Stage-2 carbonate alteration (white) in a chloritic schist (light to dark gray), showing the post-metamorphic timing of the alteration. E) Stage-2 quartz (qz)–dolomite (do)–albite (ab)–pyrite (py) veinlet crosscutting stage-2 pervasive alteration (with the same composition of the veinlet), in a microdiorite. Quartz and albite grains show undulose extinction. F) Late-stage calcite veinlet (white) crosscutting a weakly schistose and fine-grained basalt (light gray) showing a concordant layer of very fine-grained sulfide minerals (dark gray).

tures developed during a single period of progressive/incremental structural and fluid evolution. Undeformed calcite veinlets were deposited late in this evolution.

The absolute timing of deformation and gold mineralization is not constrained, but a time window can be indirectly bracketed. The minimum age of the hosting metavolcano-sedimentary succession is 2148 ± 1 Ma (Klein and Moura, 2001). Furthermore, the timing of metamorphism in the Gurupi Belt is broadly constrained by the emplacement of the peraluminous, collision-type granitoids between 2060

Ma and 2100 Ma (Palheta, 2001; Klein, 2004). Since mineralization is post-metamorphic, the age of metamorphism places an upper age limit for the mineralizing event. Moreover, preliminary Pb isotopes investigations on sulfide minerals of the Cachoeira deposit revealed Paleoproterozoic model ages around 2.0 Ga (Klein, 2004). Therefore, it is reasonable to assume that the gold mineralizing episode occurred between ~2000 and 2060 Ma. This is in agreement with the current view that these types of gold deposits form late in relation to deformation and metamorphism, at the final stages of the orogenies (e.g., Kerrich and Cassidy, 1994; Groves et al., 1998).

4. Stable isotope geochemistry

4.1. Sampling and analytical procedures

All samples were taken from drill cores of the Barbosa target, whose location is displayed in Fig. 2. Carbon, oxygen and hydrogen isotopes analyses have been performed with a Micromass Isoprime, gas-source mass spectrometer at the Laboratoire des Isotopes Stables of the Université Jean Monnet, Saint Etienne, France, whereas sulfur isotopes have been analyzed in a Finnigan MAT 252 mass spectrometer at the Stable Isotope and ICP/MS laboratory of the Queen's University, Kingston, Canada.

For carbonates, about 5 to 10 mg of dry powder (pure or mixed with silicates) were analyzed. The samples were reacted overnight in vacuum with 2 ml of 100% H_3PO_4 to produce CO_2. Calcite was reacted at 25.2 °C (McCrea, 1950), whereas dolomite was reacted at 50 °C (Al-Assam et al., 1990). The carbonate–phosphoric acid fractionation factors (Rosenbaum and Sheppard, 1986) used to recalculate the data were 1.01025 (calcite) and 1.01065 (dolomite). The extracted CO_2 was cryogenically purified. Analysis of duplicates produced agreement better than 0.24‰ for $\delta^{13}C$ and 0.25‰ for $\delta^{18}O$. Graphite was also analyzed for its carbon isotope composition using the standard off-line CuO reduction method.

Silicate minerals for oxygen and hydrogen analysis and sulfide minerals for sulfur analysis were separated by conventional magnetic and heavy liquids techniques and handpicked under binocular microscope. When carbonate minerals were present, they have been removed by reaction with HCl. All mineral separates were estimated to be >95% pure. For oxygen analysis of silicate minerals, two methods were employed, both using BrF_5 as reagent. The conventional fluorination method (Clayton and Mayeda, 1963) was employed for the hydrous minerals, and a CO_2 laser fluorination system (Harris et al., 2000), was used for quartz analysis. In the conventional method, samples were loaded into Ni-reactions tubes and degassed at 250 °C for ~2 h. Oxygen was produced by reacting 5–10 mg of samples with BrF_5 at 550 °C by 8–12 h. In the laser system oxygen was produced by heating grains weighing typically 2–4 mg with a 40 W CO_2 laser in an atmosphere of BrF_5. In both methods oxygen was converted to CO_2 by reaction with graphite, and the CO_2 was cryogenically purified. An internal standard (MONGT, $\delta^{18}O=+5.55‰$) was analyzed to calibrate the data to the SMOW scale. Duplicate analyses of three selected samples gave agreement within 0.2‰. The technique of Spicuzza et al. (1998) of rapid heating using a defocused beam was used to minimize sample loss of material during the reaction.

Hydrogen was produced by heating 10–30 mg of mineral concentrates (i.e., about 1–2 μl of H_2O) in vacuum, following procedures described in Vennemann and O'Neil (1993). The extracted H_2 was firstly converted to H_2O by passing through a CuO furnace heated at ~600 °C and purified cryogenically; the H_2O was then reduced to H_2 by reaction with "Indiana Zinc" in vacuum at 450 °C, according to procedures adapted from Coleman et al. (1982). A water standard (CTMP, $\delta D=-9‰$) was used to calibrate the data to the SMOW scale and a silicate standard (AM muscovite, $\delta D=-30‰$) furnished a mean value of −30.5‰. Inclusion fluids were extracted from ~1 to 2 g of degassed quartz by thermal decrepitation in an evacuated quartz tube heated with a gas torch to >800 °C. Hydrogen conversion followed the same procedures described for the hydrous minerals.

For sulfur analysis, SO_2 was produced from 3 to 10 mg of sulfide minerals loaded into tin capsules and reacted with CuO at 1400 °C in a He stream, using the Thermal Conversion/Elemental Analyzer — Isotope Ratio Mass Spectrometer technique. The analytical uncertainty for $\delta^{34}S$ is 0.5‰. All data are reported

in the delta notation, relative to VPDB (C), VSMOW (O and H) and VCDT (S).

4.2. Stable isotopes results

Isotope data are presented in Table 1. Eleven samples of carbonate minerals were analyzed for carbon and oxygen isotopes. One sample is from stage-3 calcite, whereas the other ten samples are from stage-2 dolomite. The $\delta^{13}C$ value of calcite is −9.8‰ and $\delta^{18}O$ is +14.2‰. The $\delta^{13}C$ and $\delta^{18}O$ values of stage-2 dolomite vary within a narrow interval, from −11.5 to −13.6‰, and from +13.4 to +15.2‰, respectively. The $\delta^{13}C$ value of the graphite carbon is −29.7‰.

The analyzed quartz samples are from veins and veinlets (stages 1 and 2), whereas chlorite and white mica were separated from the wall rock alteration (stage 2). The full range of $\delta^{18}O$ values in quartz is +14.1 to +16.9‰ ($n=10$), but most of the values are lower than +16‰ and show broadly the same range in the different hydrothermal stages (Table 1). The $\delta^{18}O$ value of chlorite is +7.9‰ and of white mica is +9.1‰, whereas their δD values are −44 and −47‰, respectively. Water extracted from fluid inclusions in a single sample showed a δD value of −22‰.

Table 1
Stable isotope results for mineral separates and inclusion fluids from the Cachoeira deposit

Paragenetic stage style	Sample no.	Host rock	Mineral	Silicates		Carbonate minerals		Fluid inclusion	Sulfide minerals
				$\delta^{18}O$ (‰)	δD (‰)	$\delta^{13}C$ (‰)	$\delta^{18}O$ (‰)	δD (‰)	$\delta^{34}S$ (‰)
1 Vein	12/107.5	Mafic tuff	Quartz	+15.9					
	15/84.5	Diorite	Quartz	+14.1					
	15/84.5	Diorite	Pyrite						+1.9
	15/84.5	Diorite	Aspy[a]						+5.7
	15/87	Diorite	Quartz	+14.8					
2 Pervasive	12/47	Microdiorite	Quartz	+16.0					
and veinlet	12/47	Microdiorite	Dolomite			−13.6	+14.4		
	12/47	Microdiorite	Pyrite						−4.2
	12/61.5	C-tuff	Graphite			−29.7			
	12/107.5	Mafic tuff	Dolomite			−11.7	+14.0		
	14/106.5	Felsic volcanic	Quartz	+15.7				−22	
	14/106.5	Felsic volcanic	Dolomite			−11.5	+13.4		
	14/106.5	Felsic volcanic	Chlorite	+7.9	−44				
	14/106.5	Felsic volcanic	White mica	+9.1	−47				
	14/108	Felsic volcanic	Pyrite						+1.9
	15/111.5	Diorite	Quartz	+15.7					
	15/111.5	Diorite	Dolomite			−12.6	+15.2		
	15/111.5	Diorite	Pyrite						+6.4
	15/112.5	Diorite	Quartz	+14.9					
	15/112.5	Diorite	Dolomite			−11.8	+14.1		
	15/112.5	Diorite	Pyrite						+4.0
	18/96.15	Microdiorite	Quartz	+16.9					
	18/96.15	Microdiorite	Dolomite			−12.3	+13.4		
	18/97.1	Microdiorite	Quartz	+15.1					
	18/97.1	Microdiorite	Dolomite			−12.4	+13.9		
	18/102	Felsic (dyke?)	Dolomite			−12.1	+14.3		
	18/102	Felsic (dyke?)	Pyrite						+2.0
	18/109	Mafic tuff	Dolomite			−12.1	+14.5		
	18/121.8	C-phyllite	Quartz	+14.7					
	18/121.8	C-phyllite	Dolomite			−11.6	+15.0		
	18/121.8	C-phyllite	Pyrite+Aspy						+2.3
3 Veinlet	18/68	Basalt	Calcite			−9.8	+14.2		

[a] Arsenopyrite.

Eight mineral separates have been analyzed for their sulfur isotope composition. The $\delta^{34}S$ values of stage-1 pyrite and arsenopyrite are +1.9‰ and +5.7‰, respectively. In stage-2, measured $\delta^{34}S$ values of pyrite are in the +1.9 to +6.4‰ range, with one single value of −4.2‰. As a whole, most of the $\delta^{34}S$ values fall within a relatively narrow range between +1.9 and +4.0‰.

4.3. Temperature and fluid composition

The geologic attributes of the Cachoeira deposit, including the metamorphic grade of the host rocks, hydrothermal assemblage, structural style, and temporal relationships between mineralization and metamorphism–deformation allow us to envisage formation temperatures between 250 and 400 °C (e.g., McCuaig and Kerrich, 1998; Mikucki, 1998; Sibson, 2004). Temperatures have been tentatively calculated using the quartz–muscovite and quartz–chlorite pairs from sample 14/106.5, and the equations of Zheng (1993). The obtained temperatures are 196 and 212 °C, respectively. These temperatures are unrealistically low, considering the geologic evidence discussed above. Petrographic observation indicates that the minerals crystallized at the same time. Therefore, these mineral pairs did not form in equilibrium, or the hydrous minerals exchanged oxygen after their formation. In fact, isotope exchange may occur even without clear petrographic evidence (Campbell and Larson, 1998), since the fine-grained white mica and chlorite are less robust in relation to quartz, which is more retentive to retrograde O-isotope exchange (Kerrich and Cassidy, 1994).

Quartz and dolomite also coexist widely in the deposit. The $\delta^{18}O$ values of carbonates partially overlap the lower values of $\delta^{18}O$ of quartz (Table 1), which is in keeping with the fractionation of carbonate–water being lower than the quartz–water. A negative covariance in the oxygen isotope composition of quartz and dolomite is observed (Fig. 7), but no relationship has been detected between this trend and any property of the mineralization, such as host rock, depth, paragenetic stage or structural style. Petrographic observations suggest that dolomite is contemporaneous with the other hydrothermal minerals in the same alteration stage, but carbonates are also susceptible to retrograde isotope exchange at temperatures lower than that of their co-precipitation with

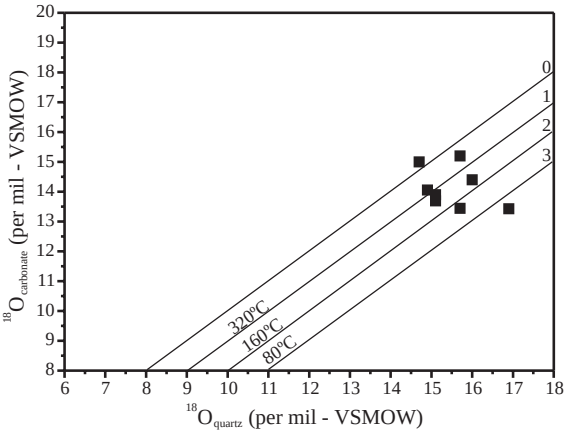

Fig. 7. Plot of $\delta^{18}O$ values of coexisting quartz and dolomite in relation to lines of equal $\delta^{18}O_{quartz}$–$\delta^{18}O_{dolomite}$. The temperatures calculated for each fractionation line (Zheng, 1999) are also shown.

quartz, even if clear petrographic evidence of disequilibrium is not detected (Brand and Veizer, 1981; Kerrich, 1987). Furthermore, the oxygen isotope fractionation between these two phases is normally large (Fig. 7), also indicating disequilibrium. On the other hand, this negative trend may also indicate change in the composition or in the temperature of the fluid from which quartz and/or dolomite were deposited. Two quartz–dolomite pairs (samples 15/112.5 and 18/97.1) yielded temperatures of 383 and 272 °C, respectively, using the oxygen isotope geothermometer of Zheng (1999). These temperatures are in agreement with the geologic evidence described above, with the range of temperatures expected for the class of gold deposits indicated for Cachoeira (see Section 5.1), and with the temperature interval of 300–386 °C that was determined for a series of gold deposits of the same class (Chega Tudo, Serrinha, Montes Áureos, and Cipoeiro) in the Gurupi Belt (Yamaguti and Villas, 2003; Klein, 2004), using fluid inclusion homogenization temperatures, chlorite chemistry, and isotope thermometry. In consequence, given the absence of a more precise result and of external geothermometer, we assume that mineralization at Cachoeira occurred within this range of 272–383 °C. It is uncertain if this interval represents the thermal (or chemical) evolution of the ore-bearing fluid. Due to the relatively restricted range of the obtained oxygen isotope values, we understand that a more restricted interval should be expected. How-

ever, this narrower interval cannot be established with the desired precision with the available data.

The full range of temperature is, nevertheless, important to estimate minimum and maximum values for the ore-fluid composition. A summary of the fluid composition is displayed in Table 2. The $\delta^{18}O_{H_2O}$ value of the fluid was calculated from the mineral analyses, using the mineral–water fractionation factors of Matsuhisa et al. (1979) for quartz, O'Neil and Taylor (1969) for muscovite, Wenner and Taylor (1971) for chlorite, and Friedman and O'Neil (1977) for carbonates. Fluid δD values were taken from the measured δD values of inclusion fluids and calculated from the hydrous minerals analysis, using the muscovite–water fractionation factor of Suzuoki and Epstein (1976) corrected according to Lambert and Epstein (1980), and the chlorite–water fractionation factor of Graham et al. (1987). The $\delta^{13}C$ value of CO_2 in the fluid was estimated from measured $\delta^{13}C$ value of carbonate minerals and the dolomite–CO_2 fractionation factor of Ohmoto and Rye (1979) and Sheppard and Schwarcz (1970). The $\delta^{34}S$ value of the fluid was calculated from the $\delta^{34}S$ value of sulfide minerals and the mineral–H_2S fractionation factor of Ohmoto and Rye (1979), assuming H_2S as the main sulfur species in the fluid. This assumption is based on the lack of oxidized phases, such as hematite and sulfate minerals, in the hydrothermal assemblage and in the host rocks, together with the determined $\delta^{34}S$ values, which indicate that the ore-bearing fluid had relatively low pH and fO_2, and that sulfide species such as H_2S prevailed during the formation of the sulfide minerals (Ohmoto and Rye, 1979; Faure, 1986).

The full range of the fluid $\delta^{18}O_{H_2O}$ values calculated from quartz is +6.2 to +12.4‰, from chlorite is +7.3 and +9.0‰, and from white mica is +5.0 and +7.5‰. The values calculated from dolomite vary between +5.9 and +11.0‰. The wide range of oxygen isotope compositions of the fluid is an artifact of the large temperature interval assumed for calculations. However, considering a single T value (lower and upper temperatures, respectively), most of the isotopic values concentrate in the +6 to +8‰ and +9.5 to +11.5‰ ranges (Fig. 8), and there is no significant

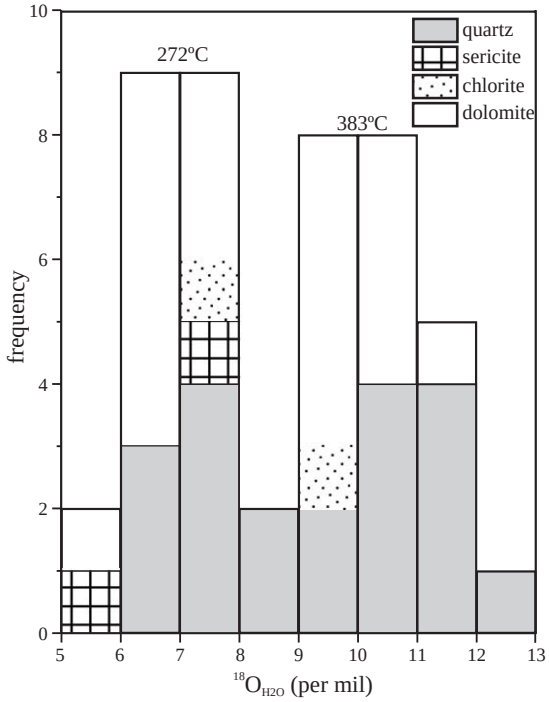

Fig. 8. Histogram showing the distribution of the oxygen isotope composition of the water in the fluid in equilibrium with different mineral phases.

Table 2
Isotopic composition of the fluid in equilibrium with minerals

Mineral	Stage	$\delta^{18}O_{H_2O}$ (‰)	δD_{H_2O} (‰)	$\delta^{13}C_{CO_2}$ (‰)	$\delta^{34}S_{H_2S}$ (‰)
Quartz	1	+6.2 to +11.4			
	2	+6.8 to +12.4			
Dolomite	2	+5.9 to +11.0		−9.5 to −12.7	
Calcite	3	+7.7 to +10.6		−7.2 to −8.1	
Chlorite	2	+7.3 to +9.0	−16		
White mica	2	+5.0 to +7.5	−20 to −28		
Fluid inclusions	2		−22		
Pyrite	1				+0.6 to +1.0
	2				−5.5 to +5.5[a]

[a] Chiefly +0.7 to +5.5.

variation between the distinct hydrothermal stages or host rocks. The δD_{H_2O} value of inclusion fluids in one single sample is −22‰, and the δD_{H_2O} values of the fluid estimated from the chlorite and white mica data are −16 and −20 to −28‰, respectively. These δD_{H_2O} values are all in good agreement.

The $\delta^{13}C$ value of fluid CO_2 was estimated to be −9.5 to −12.7‰ in stage-2 dolomite, and −7.2 to −8.1‰ in stage −3 calcite. The $\delta^{34}S$ values of H_2S assumed to be in equilibrium with the stage-1 and -2 sulfides is +0.7 to +5.5‰, with one negative value of −5.5‰.

5. Discussion

5.1. A geologic model for the Cachoeira gold deposit

Cachoeira is a shear zone-hosted gold deposit with mineralization occurring in quartz veins, quartz–carbonate veinlets and enclosing hydrothermally altered host rocks. The geologic characteristics described in this paper, including structure, host rocks (type, metamorphic grade), alteration mineralogy, mineralization style, timing of the mineralization with respect to deformation and metamorphism, and suggested tectonic setting, along with the stable isotope data, indicate that Cachoeira is similar to the class of Orogenic Gold Deposits, as defined by Groves et al. (1998). These deposits are also referred to in the literature mesothermal, mesozonal, and greenstone-hosted gold deposits. A comparison of the available data for the Cachoeira deposit with those of the neighboring gold deposits of the Gurupi Belt and of Orogenic Gold Deposits is displayed in Table 3.

5.2. Implications for fluid sources

The mineral paragenesis that resulted from the hydrothermal alteration of the volcano-sedimentary sequence is broadly constant in composition, regardless of the rock type, indicating a fluid-buffered system with a high fluid/rock ratios. A fluid-dominated system is also indicated by the lack of significant spread, for a given temperature, in the isotope composition of the fluid in equilibrium with quartz, hydrous silicates, carbonates and sulfide minerals for samples of variable depth, paragenetic stage, host rock and structural style. The overall data also suggests that the mineral phases have formed from fluids having relatively uniform oxidation state, and water and total S and C isotope compositions (Kerrich, 1987; McCuaig and Kerrich, 1998; Jia and Kerrich, 2001). Small variations in the O, H, C, and S isotope composition among the same mineral are most probably related to small-scale changes of the physico-chemical conditions during mineralization (e.g., Ohmoto, 1986).

The $\delta^{13}C$ values of carbonates and fluid of the Cachoeira deposit are not diagnostic of a unique carbon source, and are lower than the values of normal carbonates found in similar deposits (e.g., McCuaig and Kerrich, 1998). Furthermore, they are a little lower than the values of reduced carbon of igneous and metamorphic rocks and of mantle values, but they are significantly higher than the $\delta^{13}C$ values of reduced carbon of marine and organic sources (Ohmoto, 1986; Kerrich, 1987; Des Marais, 2001). The $\delta^{13}C$ value of graphite carbon is strongly negative, indicating a biogenic origin. Therefore, it is possible that this organic carbon influenced the composition of the CO_2 from which the carbonates precipitated. Accordingly, the uniform and restricted negative values of $\delta^{13}C$ have probably been generated by reaction of the CO_2 of a deep-seated (mantle-, magmatic- or metamorphic-derived) hydrothermal fluid with ^{13}C-depleted (organic) carbon near the site of ore deposition.

Combined $\delta^{18}O_{H_2O}$ and δD_{H_2O} values plot within the field of the metamorphic waters, as defined by Sheppard (1986), and are clearly outside the magmatic waters field (Fig. 9). Concerning the data on inclusion waters, we are aware that it is not conclusive. Since petrographic and microthermometrically workable fluid inclusions have not been found, it is uncertain if the extracted waters come from secondary (late?) or relic (early?) fluid inclusions. Notwithstanding, the waters of the analyzed sample have a δD value compatible with those calculated from the hydrous minerals and their compositions also plot in the metamorphic fluid field, i.e., even if the inclusions are secondary they still record the involvement of a metamorphic fluid. Furthermore, even taken into account the wide range of temperatures used to estimate fluid composition, this composition varies only within the field of the metamorphic fluid.

The total range and overall variation of the fluid $\delta^{34}S$ detected in the Cachoeira deposit (mainly 5‰)

Table 3
Comparison of selected regional- and deposit-scale characteristics of the class of orogenic gold deposits with those of Cachoeira and other gold deposits in the Gurupi Belt

Characteristics	Orogenic deposits[a,b]	Cachoeira deposit[c]	Gurupi Belt deposits[d,e]
Age	Middle Archean to Tertiary; peaks in Late Archean, Paleoproterozoic, Phanerozoic	Paleoproterozoic	Paleoproterozoic
Tectonic setting	Deformed continental margin	Deformed back-arc/continental margin	Deformed back-arc/continental margin
Structural setting/timing	Structural highs during later stages of compression and transtention	Syn- to late-tectonic (transpression)	Syn- to late-tectonic
Host rocks	Mainly mafic volcanic or intrusive rocks, or greywacke-slate sequences	Mafic volcanic and intrusive rocks, felsic volcanic rocks, tuffs, graphitic schists, phyllite	Felsic and mafic volcanic rocks, graphitic schists, pelitic schists, tonalite
Metamorphic grade of host rocks	Mainly greenschist facies (subgreenschist to lower-granulite)	Greenschist facies	Greenschist facies
Association with intrusions	Felsic to lamprophyre dykes or continental margin batholiths	Felsic dykes	Felsic dykes
Timing of mineralization	Late-tectonic, post-metamorphic peak	Syn- to late-tectonic, post-metamorphic peak	Syn- to late-tectonic, post-metamorphic peak
Mineralization style	Large veins, vein arrays, saddle reefs, replacement of Fe-rich rocks	Vein arrays and dissemination in enclosing hydrothermally-altered rocks	Vein arrays and dissemination in enclosing hydrothermally-altered rocks
Hydrothermal alteration	Mica, carbonate, Fe sulfide	Dolomite, pyrite, arsenopyrite, minor white mica and chlorite	Chlorite, white mica, calcite, pyrite
T–P conditions	Mainly 350 ± 50 °C; 1.5 ± 0.5 kbar	See text	260 to 380 °C; 1 to 4.5 kbar
Fluid composition	Low salinity, H_2O–$CO_2 \pm CH_4 \pm N_2$	Possibly H_2O–CO_2 (see text)	Low salinity, H_2O–$CO_2 \pm CH_4 \pm N_2$
Fluid oxygen and hydrogen sources	Metamorphic and/or magmatic; seldom meteoric	Metamorphic	Metamorphic (± magmatic)
Carbon and sulfur sources	C: mantle and/or magmatic and/or metamorphic, locally biogenic; S: magmatic	C: mantle and/or magmatic and/or metamorphic with biogenic contribution; S: magmatic	C: mantle and/or magmatic and/or metamorphic with biogenic contribution; S: magmatic

[a] Groves et al. (1998, 2003).
[b] McCuaig anf Kerrich (1998).
[c] This study.
[d] Yamaguti and Villas (2003), Montes Áureos deposit.
[e] Klein (2004), Cipoeiro, Chega Tudo, and Serrinha deposits.

may be considered as relatively small and normal for this type of gold deposit (McCuaig and Kerrich, 1998; Brown et al., 2003). These sulfur isotopes values may be interpreted as indicating a relatively uniform magmatic (± mantle) source, with S produced directly by magmas or by the remobilization of sulfur from magmatic rocks (Lambert et al., 1984; Kerrich, 1989), or, alternatively, as reflecting an average crustal sulfur composition. The single negative value may be attributed to some local oxidation of the fluid (Lambert et al., 1984) that can be produced by phase separation of reduced gases, or reactions of the hydrothermal fluids with ^{34}S-depleted sulfides in wall rocks (McCuaig and Kerrich, 1998; Jia and Kerrich, 2001).

5.3. Gold transport and deposition

Despite the absence of data on fluid inclusion and the chemistry of the ore fluid, and of a better definition of the temperature of ore formation, some lines of evidence can be outlined regarding parameters such as pH and redox conditions of the fluid, based on the available mineralogical and stable isotope information. These parameters help in the understanding of gold transport and deposition in the hydrothermal system of the Cachoeira deposit.

The absence of hematite or sulfate minerals in the deposit environment, the coexistence of pyrite and chlorite in the alteration assemblage, and the mea-

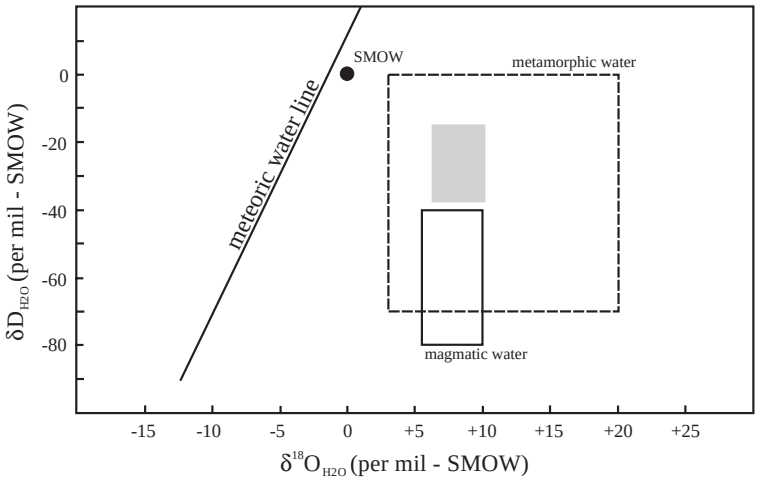

Fig. 9. Oxygen and hydrogen isotope composition of the water in the fluid in equilibrium with quartz, hydrous silicates and inclusion fluids of the Cachoeira deposit in relation to the primary magmatic and metamorphic water fields, as defined by Sheppard (1986).

sured $\delta^{34}S$ values of sulfide minerals indicate relatively reduced conditions for gold mineralization at Cachoeira (see Kerrich, 1987; Romberger, 1990; Hayashi and Ohmoto, 1991). The occurrence of white mica, carbonate, and minor albite as alteration minerals defines a near neutral to slightly alkaline nature of the mineralizing fluid (Romberger, 1990; Mikucki, 1998). At these estimated physico-chemical conditions, species such as H_2S or HS^- are the predominant sulfur species in ore fluids and, in consequence, the $Au(HS)_2^-$ was likely the gold-transporting complex (Shenberger and Barnes, 1989; Benning and Seward, 1996).

Modification of the fluid chemistry and deposition of gold follow the breakdown of the transporting sulfur complex that is caused by changes in the physico-chemical parameters, especially cooling, oxidation, increasing pH, and lowering of the amount of sulfur species in the fluid. These changes are mostly produced by fluid–rock interactions and phase separation triggered by pressure fluctuations (Shenberger and Barnes, 1989; McCuaig and Kerrich, 1998). The abundance of carbonate in the alteration assemblage is suggestive that the hydrothermal fluid was CO_2-rich. The removal of CO_2 from solution by dissociation, according to the reaction $CO_2+H_2O=H^++HCO_3^-$, raises the pH and the carbonate activity of the solution, and causes the precipitation of carbonate minerals (Rimstidt, 1997). Reaction of the fluid with the dominantly mafic host rocks (Fe-rich), allowing sulfidation, and with carbon-bearing rocks, caused changes in the redox conditions of the fluid, and probably played an important role in destabilizing gold complexes as well. Pressure fluctuations, as indicated by the coexistence of ductile and brittle features, might have also contributed.

6. Summary and concluding remarks

1) Gold mineralization in the Cachoeira deposit, Gurupi Belt, is associated with intensively sheared and fractured Paleoproterozoic metavolcano-sedimentary rocks belonging to the Chega Tudo Formation. The deposit is structurally controlled by north- and south-trending strike-slip ductile–brittle shear zones, probably related to the major Tentugal shear zone.
2) The main host rocks are mafic tuffs and diorites, although all rock types are mineralized to some extent. The hydrothermal paragenesis is syntectonic and overprints the metamorphic mineralogy of the host rocks and is mainly composed of quartz–dolomite–albite–pyrite, with subordinate amounts of chlorite, white mica and arsenopyrite. This alteration occurs both as veins and pervasively, distributed in three paragenetic stages.
3) The temperature of ore formation could not be established with precision. Estimations from mineral paragenesis, structural evidence, and oxygen

isotope thermometry are within the wide 272–383 °C range, which falls within the interval of temperatures determined in similar deposits in the Gurupi Belt and elsewhere.

4) O, H, C, and S isotope compositions of alteration minerals show restricted interval of values, indicating relatively homogeneous fluid conditions, and that mineralization occurred in a narrower temperature interval than that estimated above.
5) The isotope data are not unequivocal with respect to fluid sources. However, oxygen and hydrogen (± carbon) isotopes strongly suggest a deep-seated origin, mainly metamorphic (± magmatic, mantle-derived), with possible contamination of the fluid by organic carbon at the site of ore deposition.
6) Hydrothermal mineral assemblage, estimated temperature, and isotopic composition indicate that gold was transported as a sulfur reduced complex by a mineralizing fluid having near neutral pH and relatively low fO_2. Deposition of gold occurred in response to pH and redox reactions caused by fluid–rock interactions, phase separation, and pressure variations.
7) Geologic aspects are compatible with those described for shear zone-hosted lode gold deposits of all ages (McCuaig and Kerrich, 1998) or mesozonal orogenic gold deposits (Groves et al., 1998).

Acknowledgements

We acknowledge Antonio Ramos Bisneto and Luiz Navarro, from Brazilian International Goldfields, for field assistance and discussions on aspects of the deposit geology. Analytical support received from Christophe Renac, Frédérick Gal, and Vivianne Berthon during the analytical work at Université Jean Monnet is greatly appreciated. C. Renac is additionally acknowledged for discussions on the isotope geochemistry. The senior author benefited from funds provided by CAPES (BEX 2020/02-05), CPRM/Geological Survey of Brazil, and UFPA. The paper is a contribution to the project PRONEX/CNPq/UFPA (66.2103/1998). The authors thank two anonymous reviewers whose thoughtful comments and suggestions helped in improving this paper. **[RR]**

References

Abreu, F.A.M., Villas, R.N.N., Hasui, Y., 1980. Esboço estratigráfico do Precambriano da região do Gurupi, Estados do Pará e Maranhão. Congresso Brasileiro de Geologia, 31, Resumos expandidos, vol. 2. SBG, Camboriú, pp. 647–658.

Al-Assam, I.S., Taylor, B.E., South, B.S., 1990. Stable isotope analysis of multiple carbonate samples using selective acid extraction. Chem. Geol., Isot. Geosci. Sect. 80, 119–125.

Almeida, F.F.M., Melcher, G.C., Cordani, U.G., Kawashita, K., Vandoros, P., 1968. Radiometric age determinations from northern Brazil. Bol. Soc. Bras. Geol. 17, 3–14.

Benning, L.G., Seward, T.M., 1996. Hydrosulphide complexing of Au(I) in hydrothermal solutions from 150 to 400 °C and 500 to 1500 bars. Geochim. Cosmochim. Acta 60, 1849–1871.

Bettencourt, J.S., Borges, W.R., Koritiake, M., 1991. The Cachoeira gold deposit, Gurupi Belt, Para, Brazil: geological setting, structure and mineralization — a preliminary report. In: Ladeira, E.A. (Ed.), Brazil Gold'91. Balkema, pp. 203–208.

Brand, U., Veizer, J., 1981. Chemical diagenesis of a multi-component carbonate system: 2. Stable isotopes. J. Sediment. Petrol. 51, 987–998.

Brown, S.M., Johnson, C.A., Watling, R.J., Premo, W.R., 2003. Constraints on the composition of ore fluids and implications for mineralising events at the Cleo gold deposit, Eastern Goldfields Province, Western Australia. Aust. J. Earth Sci. 50, 19–38.

Campbell, A.R., Larson, P.B., 1998. Introduction to stable isotope applications in hydrothermal systems. In: Richards, J.P., Larson, P.B. (Eds.), Techniques in Hydrothermal Ore Deposits, Reviews in Economic Geology, vol. 6, pp. 173–193.

Clayton, R.N., Mayeda, T.K., 1963. The use of bromine pentafluoride in the extraction of oxygen from oxides and silicates from isotopic analyses. Geochim. Cosmochim. Acta 27, 43–52.

Coleman, M.L., Shepherd, T.J., Durham, J.J., Rouse, J.E., Moore, G.R., 1982. Reduction of water with zinc for hydrogen isotope analysis. Anal. Chem. 54, 993–995.

Costa, J.L., 2000. Programa Levantamentos Geológicos Básicos do Brasil. Programa Grande Carajás. Castanhal, Folha SA.23-V-C. Estado do Pará. Belém, CPRM/Geol. Surv. Brazil (CD-ROM).

Costa, J.B.S., Pastana, J.M.N., Costa, E.J.S., Jorge-João, X.S., 1988. A faixa de cisalhamento Tentugal na Folha SA.23-Y-B. Congresso Brasileiro de Geologia, XXXV, Belém, Anals, vol. 5, pp. 2257–2266.

Des Marais, D.J., 2001. Isotopic evolution of the biogeochemical carbon cycle during the Precambrian. In: Valley, J.W., Cole, D.R. (Eds.), Stable Isotope Geochemistry, Mineralogical Society of America, Reviews in Mineralogy and Geochemistry, vol. 43, pp. 555–578.

Faure, G., 1986. Principles of Isotope Geology, 2nd ed. John Wiley & Sons, New York. 589 pp.

Friedman, I., O'Neil, J.R., 1977. Compilation of stable isotope fractionation factors of geochemical interest. U.S. Geol. Surv. Prof. Paper 440-KK, 1–12.

Graham, C.M., Viglino, J.A., Harmon, R.S., 1987. Experimental study of hydrogen-isotope exchange between aluminous chlorite and water and of hydrogen diffusion in chlorite. Am. Mineral. 72, 566–579.

Groves, D.I., Goldfarb, R.J., Gebre-Mariam, M., Hagemann, S.G., Robert, F., 1998. Orogenic gold deposits: a proposed classification in the context of their crustal distribution and relationship to other gold deposit types. Ore Geol. Rev. 13, 7–27.

Groves, D.I., Goldfarb, R.J., Robert, F., Hart, C.J.R., 2003. Gold deposits in metamorphic belts: overview of current understanding, outstanding problems, future research, and exploration significance. Econ. Geol. 98, 1–29.

Harris, C., Stuart Smith, H., le Roex, A.P., 2000. Oxygen isotope composition of phenocrysts from Tristan da Cunha and Gough island lavas: variation with fractional crystallization and evidence for assimilation. Contrib. Mineral. Petrol. 138, 164–175.

Hasui, Y., Abreu, F.A.M., Villas, R.N.N., 1984. Província Parnaíba. O Pré-Cambriano no Brasil. Edgard Blücher, pp. 36–45.

Hayashi, K.I., Ohmoto, H., 1991. Solubility of gold in NaCl- and H_2S-bearing aqueous solutions at 250–350 °C. Geochim. Cosmochim. Acta 55, 2111–2126.

Hurley, P.M., Melcher, G.C., Pinson, W.H., Fairbairn, H.W., 1968. Some orogenic episodes in South America by K–Ar and whole-rock Rb–Sr dating. Can. J. Earth Sci. 5, 633–638.

Jia, Y., Kerrich, R., 2001. Stable isotope (O, H, S, C, and N) systematics of quartz vein systems in the turbidite-hosted Central and North Deborah gold deposits of the Bendigo Gold Field, Central Victoria, Australia: constraints on the origin of ore-forming fluids. Econ. Geol. 96, 705–721.

Kerrich, R., 1987. The stable isotope geochemistry of Au–Ag vein deposits in metamorphic rocks. In: Kyser, T.K. (Ed.), Stable Isotope Geochemistry of Low Temperature Fluids, Short Course, vol. 13. Mineralogical Association of Canada, pp. 287–336.

Kerrich, R., 1989. Geochemical evidence on the sources of fluids and solutes for shear zone hosted mesothermal Au deposits. In: Bursnall, J.T. (Ed.), Mineralization and Shear Zones, Short Course Notes, vol. 6. Geol. Assoc. Canada, pp. 129–197.

Kerrich, R., Cassidy, K.F., 1994. Temporal relationships of lode gold mineralization to accretion, magmatism, metamorphism and deformation — Archean to present: a review. Ore Geol. Rev. 9, 263–310.

Klein, E.L., 2004. Evolução geologica pré-cambriana e aspectos da metalogênese do ouro do Craton São Luis e do Cinturão Gurupi, NE-Para/NW-Maranhão, Brasil. Unpub. DSc Thesis, Universidade Federal do Pará, Belém, Brazil.

Klein, E.L., Moura, C.A.V., 2001. Age constraints on granitoids and metavolcanic rocks of the São Luis Craton and Gurupi Belt, northern Brazil: implications for lithostratigraphy and geological evolution. Int. Geol. Rev. 43, 237–253.

Klein, E.L., Moura, C.A.V., 2003. Síntese geólogica e geocronológica do Craton São Luis e do Cinturão Gurupi na região do rio Gurupi (NE-Para/NW-Maranhão). Revista Geologia USP, Série Cientifica 3, 97–112.

Lambert, S.J., Epstein, S., 1980. Stable isotope investigations of an active geothermal system in Valles Caldera, Jemez Mountains, New Mexico. J. Volcanol. Geotherm. Res. 8, 111–129.

Lambert, I.B., Phillips, G.N., Groves, D.I., 1984. Sulfur isotope compositions and genesis of Archaean gold mineralization, Australia and Zimbabwe. In: Foster, R.P. (Ed.), Gold'82: The Geology, Geochemistry and Genesis of Gold Deposits. Geological Society of Zimbabwe Special Publication 1, pp. 373–387.

Matsuhisa, Y., Goldschmit, J.R., Clayton, R.N., 1979. Oxygen isotope fractionation in the system quartz–albite–anorthite–water. Geochim. Cosmochim. Acta 43, 1131–1140.

McCrea, M., 1950. The isotopic chemistry of carbonates and a paleotemperature scale. J. Chem. Phys. 18, 849–857.

McCuaig, T.C., Kerrich, R., 1998. *P–T–t*–deformation–fluid characteristics of lode gold deposits: evidence from alteration systematics. Ore Geol. Rev. 12, 381–453.

Mikucki, E., 1998. Hydrothermal transport and depositional processes in Archaean lode–gold systems: a review. Ore Geol. Rev. 13, 307–321.

Ohmoto, H., 1986. Stable isotope geochemistry of ore deposits. In: Valley, J.W., Taylor Jr., H.P., O'Neil, J.R. (Eds.), Stable Isotopes in High Temperature Geological Processes, Reviews in Mineralogy, vol. 16. Mineral. Soc. America, pp. 491–559.

Ohmoto, H., Rye, R.O., 1979. Isotopes of sulfur and carbon. In: Barnes, H.L. (Ed.), Geochemistry of Hydrothermal Ore Deposits. Jon Wiley & Sons, pp. 509–567.

O'Neil, J.R., Taylor, H.P., 1969. Oxygen isotope equilibrium between muscovite and water. J. Geophys. Res. 74, 6012–6022.

Palheta, E.S.M., 2001. Evolução geológica da região nordeste do Estado do Pará com base em estudos estruturais e isotópicos de granitóides. Unpub. MSc thesis, Universidade Federal do Pará, Belém, Brazil.

Pastana, J.M.N., 1995. Programa Levantamentos Geológicos Básicos do Brasil. Programa Grande Carajás. Turiaçu/Pinheiro, folhas SA.23-V-D/SA.23-Y-B. Estados do Pará e Maranhão. CPRM, 205 pp.

Pinheiro, B.L.S., Moura, C.A.V., Klein, E.L., 2003. Estudo de proveniência em arenitos das formações Igarapé de Areia e Viseu, nordeste do Pará, com base em datação de monocristais de zircão por evaporação de chumbo. Simposio de Geologia da Amazônia, vol. 8. Resumos expandidos, Manaus. (CD-ROM).

Ribeiro, J.W.A., 2002. O arcabouço estrutural da região de Chega Tudo e Cedral, NW do Maranhão, com base em sensores geofisicos. Unpub. MSc thesis, Universidade Federal do Pará, Belém, Brazil.

Rimstidt, J.D., 1997. Gangue mineral transport and deposition. In: Barnes, H.B. (Ed.), Geochemistry of Hydrothermal Ore Deposits. J. Wiley & Sons, pp. 487–515.

Romberger, S.B., 1990. Transport and deposition of gold in hydrothermal systems. In: Robert, F. (Ed.), Greenstone Gold and Crustal Evolution NUNA conference, pp. 61–66.

Rosenbaum, J., Sheppard, S.M.F., 1986. An isotopic study of siderites, dolomites and ankerites at high temperatures. Geochim. Cosmochim. Acta 50, 1147–1150.

Shenberger, D.M., Barnes, H.L., 1989. Solubility of gold in sulfide solutions from 150 to 350 °C. Geochim. Cosmochim. Acta 53, 269–278.

Sheppard, S.M.F., 1986. Characterization and isotopic variations in natural waters. In: Valley, J.W., Taylor Jr., H.P., O'Neil, J.R. (Eds.), Stable Isotopes in High Temperature Geological Processes, Reviews in Mineralogy, vol. 16. Mineral. Soc. America, pp. 165–184.

Sheppard, S.M.F., Schwarcz, H.P., 1970. Fractionation of carbon and oxygen isotopes and magnesium between coexisting metamorphic calcite and dolomite. Contrib. Mineral. Petrol. 26, 161–198.

Sibson, R.H., 2004. Controls on maximum fluid overpressure defining conditions for mesozonal mineralisation. J. Struct. Geol. 26, 1127–1136.

Spicuzza, M.J., Valley, J.W., Kohn, M.J., Girard, J.P., Fouillac, A.M., 1998. The rapid heating, defocused beam technique: a CO_2-laser-based method for highly precise and accurate determination of $\delta^{18}O$ values of quartz. Chem. Geol. 144, 195–203.

Suzuoki, T., Epstein, S., 1976. Hydrogen isotope fractionation between OH-bearing minerals and water. Geochim. Cosmochim. Acta 40, 1229–1240.

Trarbach, M., Kotschoubey, B., 1991. Estudo do comportamento do ouro nas lateritas ferruginosas e corpos gossânicos da região de Cachoeira, nordeste do Estado do Para. Simposio de Geologia da Amazônia, 3, Belém. Extended abstracts, pp. 584–595.

Vennemann, T.W., O'Neil, J.R., 1993. A simple and inexpensive method for hydrogen isotope and water analyses of minerals and rocks based on zinc reagent. Chem. Geol., Isot. Geosci. Section 103, 227–234.

Villas, R.N.N., 1982. Geocronologia das intrusões ígneas na bacia do rio Guamá, nordeste do Estado do Pará. Simpósio de Geologia da Amazônia, 2, Belém, vol. 1, pp. 233–247.

Wenner, D.B., Taylor Jr., H.P., 1971. Temperatures of serpentinization of ultramafic rocks based on $^{18}O/^{16}O$ fractionation between coexisting serpentine and magnetite. Contrib. Mineral. Petrol. 32, 165–168.

Yamaguti, H.S., Villas, R.N.N., 2003. Estudo microtermométrico dos fluidos hidrotermais relacionados com a mineralização aurífera de Montes Áureos, NW do Maranhão. Rev. Bras. Geociênc. 33, 21–32.

Zheng, Y.F., 1993. Calculation of oxygen isotope fractionation in hydroxyl-bearing silicates. Earth Planet. Sci. Lett. 120, 247–263.

Zheng, Y.F., 1999. Oxygen isotope fractionations in carbonate and sulfate minerals. Geochem. J. 33, 109–126.